Characterization of Mixed Micelles of SDS and a Sugar-Based Nonionic Surfactant as a Variable Reaction Medium

Barney L. Bales* and Radha Ranganathan

Department of Physics and Astronomy and the Center for Supramolecular Studies, California State University at Northridge, Northridge, California 91330-8268

P. C. Griffiths

Department of Chemistry, Cardiff University, CF10 3TB United Kingdom

Received: March 12, 2001; In Final Form: May 30, 2001

Time-resolved fluorescence quenching (TRFQ), electron paramagnetic resonance (EPR), and small-angle neutron scattering (SANS) are employed to characterize mixed micelles of sodium dodecyl sulfate (SDS) and the nonionic sugar-based surfactant dodecylmalono-bis-*N*-methylglucamide (DBNMG) as a reaction medium. Interpretation of the results from the three methods are constrained to fit the classical model of a hydrocarbon core surrounded by a polar shell. As measured by TRFQ, at 45 °C, the aggregation numbers increase from 48 for pure SDS to a maximum of 63 at 36 mole percent DBNMG and decrease again to 49 for pure DBNMG. The aggregation numbers of the pure DBNMG increase from 33 at 21 °C to 49 at 45 °C. SANS results of the pure DBNMG are interpreted by fixing the aggregation number at 49 (from TRFQ) and allowing the polar shell thickness to vary as a fitting parameter, yielding a value of 5.8 Å at 45 °C. EPR, utilizing a hydrophobic spin probe, is used to measure the nonempirical polarity index, H(25 °C), of the polar shell. H(25 °C) is defined to be the ratio of molar concentration of OH dipoles in a solvent or solvent mixture to that in water at 25 °C; thus, both water and the sugar headgroups contribute. By fixing the volume in the polar shell inaccessible to water due to the presence of SDS (127 Å^3) and DBNMG (580 Å^3), theoretical values of H(25 °C) are computed, the result depending only on the number of OH bonds in DBNMG available to interact with the spin probe. A constant average value of 7.4 OH bonds out of a maximum possible number of 10 reproduces the measured values over the full range of mixed micelle compositions. At 45 °C, the microviscosity of the polar shell, as deduced from the rotational correlation time of the spin probe, varies from 2.79 ± 0.05 cP for pure SDS to 13.1 ± 0.2 cP for pure DBNMG departing only slightly from a linear dependence on the mole fraction of DBNMG. The uncertainties in the viscosity are the standard deviations in 10 measurements and therefore represent the uncertainty in the relative values of the viscosity. The viscosity decreases from 32 ± 4 cP at 21 °C to 13.1 ± 0.2 cP at 45 °C for pure DBNMG micelles. These viscosities are used to show that the quenching rate constant of pyrene by dimethyl benzophenone, measured by TRFQ, follows the Stokes−Einstein−Smolukhovsky equation with a quenching probability of $P = 0.5$ whether the mixed micelle composition is changed at constant temperature or if the temperature is varied in pure DBNMG. The volume of the polar shell enters into the formulation because the effective concentration of the quencher depends on that volume; however, the quenching rates are not correlated with volume alone.

Introduction

A considerable amount of basic research has attempted to characterize micelles as reaction media.[1,2] Mixed micelles are particularly interesting since these potentially offer the possibility to tune the reaction medium by adjusting their composition.[3−7] Progress in achieving a deep understanding of the physicochemical properties of micelles has been limited,[2] because an understanding of both the structural and the dynamic properties must be achieved simultaneously. There does not exist a single technique capable of yielding both types of information unambiguously; thus, there is a need to combine techniques in order to increase the information and thereby decrease the uncertainties. In this work, we combine electron paramagnetic resonance (EPR), time-resolved fluorescence quenching (TRFQ), and small-angle neutron scattering (SANS) techniques to study mixed micelles of sodium dodecyl sulfate (SDS) and dodecylmalono-bis-*N*-methylglucamide (DBNMG).

We have been investigating[8−10] mixed micelles of SDS and DBNMG using a variety of techniques. In this work, we add TRFQ as a technique and extend our study to include the entire composition range, $X = 0$ to 1, where

$$X = \frac{[\text{DBNMG}]}{[\text{DBNMG}] + [\text{SDS}]} \tag{1}$$

is the stoichiometric mole fraction of DBNMG.

For an overview of mixed micelles in general, see refs 11,-12. For a discussion of the behavior of DBNMG/SDS mixtures at low concentrations, see ref 8. As discussed in ref 10, at the 50-mM total surfactant concentration employed in this study, the micellar and stoichiometric compositions are the same to

* Corresponding author. E-mail: barney.bales@email.csun.edu.

10.1021/jp010941d CCC: $20.00
Published on Web 00/00/0000 PAGE EST: 8.6

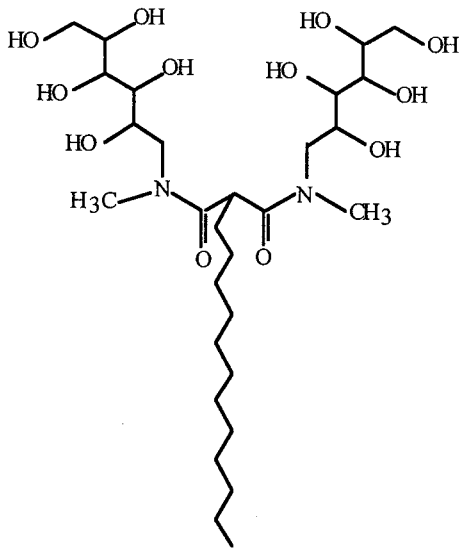

DBNMG

within a few percent. Thus, we may use the simplified notation of eq 1 to denote the micelle composition as well.

In this work, we interpret the results of three techniques in the framework of a classical micelle model with a spherical hydrocarbon core and polar shell. We constrain the interpretation of the three methods to agree with one model and one another as follows: the aggregation number of the mixed micelle is constrained to be that measured by TRFQ. The thickness of the polar shell is found by SANS fixing the aggregation number. The theoretical value of the hydration of the micelle is calculated from a simple geometrical model and compared with the experimental results derived from EPR.

The viscosity of the polar shell is deduced from measurements of the rotational correlation time of a spin probe as the micelle composition or the temperature are varied. These viscosities are used to show that the quenching rate constant of pyrene by dimethyl benzophenone, measured by TRFQ, follows a classical hydrodynamic description.

Methods and Materials

The nonionic surfactant DBNMG (U.S. Patent 5,298,191) was a kind gift from A. M. Howe and A. R. Pitt of Kodak European R&D. It was purified by HPLC using a reverse phase column as described in detail previously.[10] Sodium dodecyl sulfate (SDS) and the spin probe 16 doxyl-stearic acid methyl ester (16DSE) from Sigma and dimethyl benzophenone (DMBP) from Aldrich were used as received. Pyrene (Aldrich) was purified by recrystallization from ethanol. MilliQ water was used as the solvent for the surfactant solutions.

Small-angle neutron scattering (SANS) investigations of DBNMG/SDS mixed micelles have been previously reported,[8] but subsequent work has shown that the nonionic material used in that original work contained a small amount of an anionic impurity. We have therefore purified DBNMG with HPLC as described in detail [10] and remeasured the scattering data for pure 50-mM DBNMG ($X = 1$). The SANS measurements were performed at 45 °C on the fixed-geometry, time-of-flight LOQ diffractometer at the ISIS Spallation Neutron Source, Oxfordshire, U.K. Neutron wavelengths between 2 and 10 Å were utilized, such that a Q-range of approximately 0.008 to 0.22 $Å^{-1}$ can be accessed. Further experimental details are identical to those described previously.[8]

Samples for TRFQ measurements were prepared as follows. Stock solutions of pyrene (25 mM) and the quencher DMBP (10 mM) were prepared in ethanol and stored in a freezer until needed. An aliquot of the pyrene stock solution sufficient to provide an approximate pyrene/surfactant molar ratio 1:5000 was added to a vial and the solvent evaporated by a slow stream of dry nitrogen gas. A 50-mM solution of SDS was added to this vial and was gently stirred for 24 h. A 50-mM solution of DBNMG containing pyrene was similarly prepared. An aliquot of the DMBP solution was added to a vial and the solvent evaporated by a slow stream of dry nitrogen gas. A portion of the pyrene−SDS solution, sufficient to provide a DMBP/surfactant molar ratio of 1.00:23.3, was added to this vial and stirred gently for 12 h. A solution containing pyrene, DMBP, and DBNMG was similarly prepared. By mixing combinations of SDS and DBNMG solutions with and without DMBP, samples at various values of X and various concentrations of the quencher were prepared all having the same concentration of pyrene as detailed in Tables 2−5. Dilution of the $X = 1$, 50-mM solution with water yielded the samples at lower DBNMG concentrations detailed in Table 4.

Fluorescence decay data were accumulated using the time-correlated single-photon counting technique using a mode-locked Nd:YAG laser (Spectra Physics 3800/451) pumping a cavity-dumped DCM-dye laser (Spectra Physics 3500/454). using procedures identical to those reported previously.[13] Briefly, the decay curves were fit to the Infelta−Tachiya equation,[14,15] yielding, as expected, parameters consistent with negligible migration of the quencher during the lifetime of the pyrene fluorescence. The fits yield the average number of quenchers per micelle, ⟨N⟩, and the rate of quenching due to one quencher, k_q. The assumptions involved in this analysis have been exhaustively discussed in the literature to which the reader is referred.[14−16]

From the average number of quenchers per micelles, the average aggregation number, N, may be computed as follows:

$$N = \langle N \rangle / \eta_Q \tag{2}$$

where the scaled quencher concentration, η_Q, is given by

$$\eta_Q = \frac{[Q]}{[\text{surfactant}] - [\text{surfactant}]_{\text{free}}} \tag{3}$$

The square brackets indicate molar concentrations, the subscript "free" indicates the surfactant concentration in monomer form, and Q is the quencher, in this case, DMBP. For $X = 0$, pure SDS, $[\text{surfactant}]_{\text{free}}$ was calculated from eq 5 of ref 17 and for $X > 0$, from Rubingh's regular solution theory[18] using cmc data of the mixed micelles.[8] These values appear in Table 5.

Experimental details for the EPR measurements are identical to those described previously;[10] essential details are repeated here. Two stock solutions of 50-mM DBNMG and 50-mM SDS with spin−probe/surfactant molar ratios of 1:400 were prepared and mixed with one another to yield varying compositions $X =$ 0 to 1. The 50-mM solution of DBNMG was diluted with distilled water to yield concentrations [DBNMG] = 20−50 mM. The samples, not degassed, were sealed with a gas−oxygen torch into melting point capillaries which were housed within a quartz EPR tube for the measurements. The temperature was controlled to about ±0.2 K by the Bruker Variable Temperature Unit BVT 2000 and was measured with a thermocouple before and after the spectra were taken. The uncertainty in the temperature is estimated to be ±1 °C.

Five spectra were taken one after the other at X-band with a Bruker ESP-300 spectrometer. The spectra were transferred to a PC and fit with the program LOWFIT, coded in C, which fits the experimental lines to approximate Voigt line shapes.[19,20] This separates the Gaussian and Lorentzian components of the spectral lines and locates the resonance fields of the three EPR lines to a precision of a few mG.

Rotational correlation times are computed from the following well-known formulas (see, for example ref 21 and references therein).

$$C_{\text{uncorrected}} = \frac{1}{2}\Delta H^0_{\text{pp}_0}\left\{\sqrt{\frac{V_{\text{pp}_0}}{V_{\text{pp+1}}}} + \sqrt{\frac{V_{\text{pp0}}}{V_{\text{pp-1}}}} - 2\right\} \quad (4)$$

$$B_{\text{uncorrected}} = \frac{1}{2}\Delta H^0_{\text{pp}_0}\left\{\sqrt{\frac{V_{\text{pp}_0}}{V_{\text{pp+1}}}} - \sqrt{\frac{V_{\text{pp}_0}}{V_{\text{pp-1}}}}\right\} \quad (5)$$

where $\Delta H^0_{\text{pp}_0}$ is the overall line width of the $M_I = 0$ line and V_{ppM_I} is the peak-to-peak height of the M_I line, where $M_I = 1$, 0, -1 labels the low-, center-, and high-fields lines, respectively. The subscript "uncorrected" means that the coefficients have not yet been corrected for inhomogeneous broadening, which is carried out using eqs 28−30 of ref 20. From corrected coefficients, rotational correlation times may be computed[22] from

$$\tau_B = -1.27 \times 10^{-9} B_{\text{corrected}} \quad (6)$$

$$\tau_C = 1.16 \times 10^{-9} C_{\text{corrected}} \quad (7)$$

where τ_B, τ_C are given in seconds, and $B_{\text{corrected}}$, $C_{\text{corrected}}$, in Gauss. The derivation of eqs 6 and 7 require that the rotational averaging of the g- and hyperfine-tensors be isotropic, which would require that $\tau_B = \tau_C$, and that τ_B, τ_C be <3 ns. See ref 21 and the references therein for a careful discussion of the validity of these expressions and for details of their derivation. We have departed slightly from the procedure of ref 21 by using the tensor elements derived from 5 doxylstearic acid immobilized on lyophilized bovine serum albumin[23] rather than those for 1-oxyl-2,2,4,4-tetramethyloxazolidine, studied as an impurity in a single-crystal environment.[24]

Theory

Model of DBNMG/SDS Micelles. We employ the same model previously used to interpret TRFQ and EPR data in SDS and lithium dodecyl sulfate micelles.[25,26] The model is based on a classical picture of the micelle as having a hydrocarbon core with very little water penetration[27] surrounded by a polar shell. The inner spherical hydrocarbon core has a radius, R_c, that is determined by the volume of the surfactant alkyl chains. The volume of the core is taken to be NV_{tail}, where N is the aggregation number and $V_{\text{tail}} = 350$ Å^3 is the volume occupied by the saturated hydrocarbon chain[28]). Thus the core radius is found from

$$NV_{\text{tail}} = \frac{4\pi}{3}R_c^{\,3} \quad (8)$$

The volume in the polar shell, V_{shell}, is given by

$$V_{\text{shell}} = \frac{4\pi}{3}(R_m^{\,3} - R_c^{\,3}). \quad (9)$$

Fixing the shell thickness $R_m - R_c$ from SANS measurements yields the micelle radius, R_m, from which the micelle volume may be calculated

$$V_{\text{micelle}} = \frac{4\pi}{3}R_m^{\,3} \quad (10)$$

See the details of the assumptions and the calculations in ref 25.

We have persisted with the core−shell model for the nonionic micelles because the data from the three methods fit the model so well. If further work reveals that the model needs to be modified, then the above formulation would need modification. The details of the modification would depend on the alternate model.

Microviscosity from EPR Measurements of the Rotational Correlation Time. The microviscosity of the environment of a spin probe may be estimated by measuring its rotational correlation time and utilizing the Debye−Stokes−Einstein equation[29]

$$\tau = 4\pi\eta R^3/3kT \quad (11)$$

where η is the shear viscosity of the solvent, k the Boltzmann constant, T the absolute temperature, and R the hydrodynamic radius of the molecule. The important question of the application of eq 11 to molecules of dimensions comparable to those of the solvent was discussed in detail in ref 22 and in the large literature referenced therein.[22] The conclusion is that eq 11 holds in the sense that the rotational correlation time varies linearly with η/T whether T, and thus η, are varied or whether η is varied by hydrostatic pressure.[22] The value of R in eq 11 often does not correspond accurately to the geometrical value computed from van der Waals radii, for example, by the method of Bondi;[30] however, if R is constant as the solvent, temperature, and viscosity are changed, then eq 11 may be used to measure viscosity.

A procedure to apply the technique to a micelle was described in ref 22 which may be consulted for details on the background, assumptions, and procedures.

To estimate the microviscosity from rotational correlation times measured in the laboratory frame of reference, the overall motion of the doxyl group is modeled as a reorientation relative to the micelle as a unit with rotational correlation time τ_{relative} and an isotropic reorientation of the micelle as a whole at τ_{micelle}. These reorientations are assumed to be independent, so

$$\frac{1}{\tau_C} = \frac{1}{\tau_B} = \frac{1}{\tau_{\text{relative}}} + \frac{1}{\tau_{\text{micelle}}} \quad (12)$$

τ_{micelle} is computed from the Debye−Stokes−Einstein equation written as follows:

$$\tau_{\text{micelle}} = V_{\text{micelle}} \times \frac{\eta}{kT}, \quad (13)$$

where V_{micelle} is found from eq 10 and η is the viscosity of pure water.[31]

Hydrodynamic Description of Bimolecular Collisions in Micelles. To be definite, we frame the discussion in terms of the quenching rate of the fluorescence of the probe by the quencher; however, it will be recognized that the discussion will apply to other rates as well; for example, chemical reaction rates, and spin exchange rates between paramagnetic particles. The rate k_q is proportional to the concentration of the quencher in the polar shell, C_Q,

$$k_q = C_Q P K_D \tag{14}$$

where K_D is the collision rate constant and P is the probability that quenching occurs upon collision. If the concentration is expressed in mol/L, then the rate constant K_D has units l/mol·s. Since k_q is the quenching rate due to one quencher, then C_Q is the molar concentration of one molecule in the volume V_{shell}. One molecule is N_0^{-1} moles of quencher, where N_0 is Avogadro's number, so

$$C_Q = \frac{10^{27}}{N_0 V_{shell}} \tag{15}$$

The factor 10^{27} converts the volume V_{shell} from Å^3 to liters.

A hydrodynamic description of bimolecular collision rates between the probe and the quencher in liquids is based upon combining the Smolukhovsky and the Stokes−Einstein equations to yield the well-known expression[32] for the diffusional collision rate constant

$$K_D = \frac{8kT}{3\eta}. \tag{16}$$

Converting eq 16 to units l/mol·s yields

$$K_D = \frac{8R_0T}{3000\eta} \tag{17}$$

where $R_0 = 8.31 \times 10^7$ erg/deg is the gas constant and η has unit Poise. Despite the fact that its derivation employs some radical assumptions, eq 17 is surprisingly accurate in its description of collisions between nonspherical molecules diffusing in solvents comprised of comparably sized molecules. Equation 17 has been critically and exhaustively discussed in the literature.[32−34] We pose the question: can eq 17 describe the collision rates of molecules diffusing in the polar shell of micelles with the level of success previously found in bulk liquids? A remarkable feature of eq 17 is its independence of the size of the diffusing molecules; in Debye's words[32] "a peculiar but well-known result in colloid chemistry". Thus all quenchers and probes would collide with the same rate constant.

Combining eqs 14 and 17

$$k_q = P C_q \frac{8R_0T}{3000\eta} \tag{18}$$

It is well-known that the fluorescence quenching rate often varies inversely with the size of micelles.[35] Proposed size dependences have varied from $1/V$ to $1/V^{2/3}$ depending on whether the molecules are envisioned to diffuse in 3- or 2-dimensions.[35] Such proposals ignore the influence of the viscosity on the diffusion, in effect, tacitly assuming that the viscosity is more or less the same as the micelle size is varied.

Results

EPR Results. Three-line narrow EPR spectra of 16DSE typical of nitroxide-free radicals undergoing approximately isotropic motion in the motional narrowing region were observed for all samples. See, for example, Figure 1a of ref 25. The difference in resonance fields between the center and low-field lines, A_+, given in Gauss, has been shown[25,26] to vary linearly with the nonempirical polarity index,[36] H(25 °C), as follows:[10]

$$A_+ = 14.309 + 1.418\, H(25\ °C), \tag{19}$$

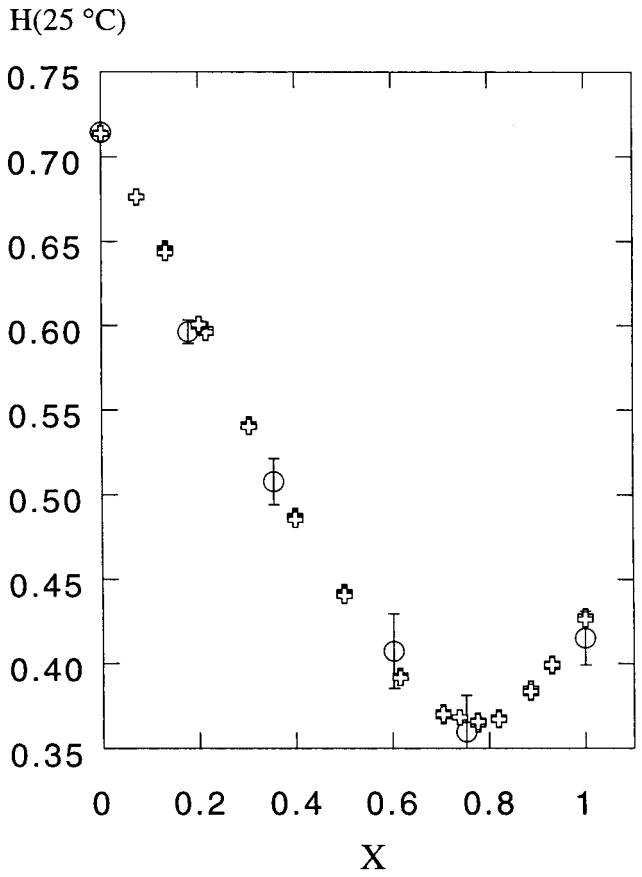

Figure 1. Polarity index, H(25°C), versus mole fraction of DBNMG, X. Measurements from EPR (open crosses) and theoretical (○) employing $V_{DBNMG} = 580 \pm 10$ and $N_{OH} = 7.4 \pm 0.2$. Error bars are computed from the uncertainties due to V_{DBNMG} and N_{OH} added in quadrature. The initial decline in the polarity is due to a net loss in OH bonds in the polar shell as water is expelled faster than OH bonds from the entering sugar groups replace them. Near $X = 0.75$ the polar shell becomes free of water and the increase above this point is due to OH bonds entering the polar shell on the sugar groups.

where H(25 °C) is defined to be the ratio of molar concentration of OH dipoles in a solvent or solvent mixture to that in water.[36]

Hyperfine spacings A_+ were measured and eq 19 employed to yield values of the polarity index H(25 °C). These are plotted, as open crosses, versus mixed micelle composition in Figure 1. The values of H(25 °C) for $X < 0.3$ are in agreement with those previously published.[10] At higher values of X the polarity index reaches a rather low value of 0.37 near $X = 0.75$, confirming a prediction[10] of a rather dry mixed micelle, and above this value of X, the value of H(25 °C) increases. The open circles are the theoretical prediction of the polarity index discussed below.

To estimate the microviscosity of the polar shell of mixed micelles, we apply eq 11, where the pertinent rotational correlation time is $\tau_{relative}$, eq 12. To proceed, we need the hydrodynamic radius of the spin probe 16DSE which has not been determined previously. For flexible spin probes such as the doxyl labeled fatty acids and their methyl esters, much of the rotational mobility of the doxyl groups derives from intramolecular motion. Thus one finds that these molecules have an intrinsic flexibility[37] which means that the value of R determined from eq 11 by measuring the rotational correlation time in a solvent of known viscosity depends on the position of the doxyl group within the spin probe. The critical issue is whether R remains constant for a given spin probe. Yoshioka[38] has shown this to be so for some stearate nitroxides as the temperature is varied. Here we show that R is also constant as

TABLE 1: Hydrodynamic Radius of 16DSE, $R = 3.75 \pm 0.08$ Å. $T = 25$ °C

X_{MeOH}, wt %	η, cP[a]	$R(\tau_B)$[b], Å	$R(\tau_C)$[c], Å
0.41	1.60	3.75± 0.07	3.81± 0.04
0.57	1.47	3.66± 0.01	3.66± 0.02
0.68	1.28	3.69± 0.02	3.65± 0.02
0.78	1.07	3.74± 0.02	3.67± 0.03
0.88	0.84	3.86± 0.14	3.78± 0.15
0.98	0.59	3.91± 0.08	3.75± 0.05
1.00	0.55	3.73± 0.12	3.83± 0.14
mean		3.76± 0.07	3.74± 0.09

[a] Ref 39. [b] Calculated from eq 11 from values of τ_B. [c] Calculated from eq 11 from values of τ_C. Errors are standard deviations in five measurements using the same sample.

the viscosity is varied by changing the solvent composition. This has been carried out by using methanol−water mixtures spanning the same range of values of H(25 °C) as is found in the micelles. These spectra were already available from previous work.[10] From each spectrum, values of the coefficients in eqs 4 and 5 were calculated and corrected using eqs 28−30 of ref 20. Rotational correlation times τ_B and τ_C were calculated from eqs 6 and 7. The viscosity of these reference mixtures were found by linear interpolation between handbook values.[39] Inserting the rotational correlation times, τ_B and τ_C, respectively, and the viscosities into eq 11 yield values of the hydrodynamic radii $R(\tau_B)$ and $R(\tau_C)$ which are presented in Table 1. The uncertainties are standard deviations of 5 measurements using the same sample. Table 1 shows that the hydrodynamic radius of 16DSE is independent of viscosity. Averaging over the range of viscosities in Table 1 yields hydrodynamic radii $R(\tau_B) = 3.76 \pm 0.07$ Å and $R(\tau_C) = 3.74 \pm 0.09$ Å where the uncertainty is the unweighted standard deviation over the 7 values of viscosity. The fact that these two values are equal shows that 16DSE satisfies the requirement of eqs 6 and 7 for isotropic motion. We average $R(\tau_B)$ and $R(\tau_C)$ to arrive at the hydrodynamic radius for 16DSE $R = 3.75 \pm 0.08$ Å.

One attractive feature in using 16DSE to study micelles is that one avoids the uncertainty associated with some spin probes in which τ_B and τ_C are not equal. Particularly troublesome in this regard is 5 doxylstearic acid which not only yields different values of τ_B and τ_C but also is sensitive to changes in the pH.[40]

The rotational correlation times of the micelles were calculated from eq 13 using the viscosity of pure water and the values of $\tau_{relative}$ were found from eq 12. Inserting $\tau_{relative}$ into eq 11 yielded the values of the viscosity of the polar shell of the mixed micelles which are plotted in Figure 2 versus the mixed micelle composition X. The viscosity increases by a factor of more than four even though the aggregation number varies only modestly. Note that an error in value of the hydrodynamic radius for 16DSE would contribute a systematic error to Figure 2, raising or lowering all of the values. The relative values would be but little affected.

TRFQ. All of the fluorescence decay curves observed in this study were typical curves well fit by the Infelta−Tachiya equation, similar, for example, to Figure 1 of ref 41. We recall that a rigorous application of the analysis requires that the micelles be monodisperse and that the quenchers are distributed randomly among the micelles. A necessary consequence of these assumptions is that the value of N be independent of the quencher concentration. Table 2 shows the results of varying the quencher concentration in DBNMG micelles, $X = 1$ at $T =$ 21 °C. Values of the aggregation numbers and quenching rate constants are independent of the quencher concentration supporting the assumptions of a Poisson distribution and a small micelle size dispersion.

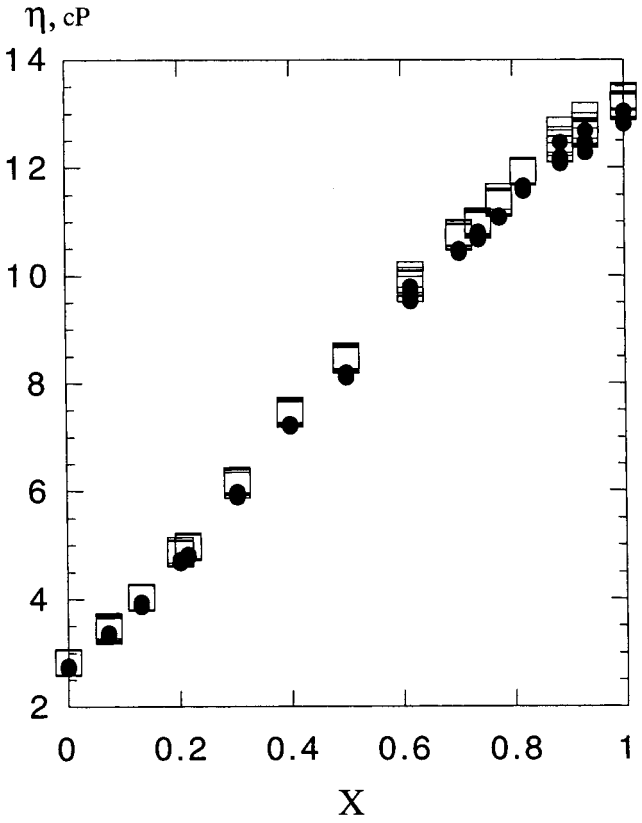

Figure 2. The microviscosity of the polar shell of mixed micelles as a function of micelle composition. Individual symbols are from different measurements. The squares denote values deduced from τ_C and solid circles from τ_B. Isotropic motion is indicated by the equivalence $\tau_C = \tau_B$.

TABLE 2: Effect of Quencher Concentration on the Aggregation Number of 50 mM DBNMG Micelles. $T = 21$ °C

[DMBP], mM	η_Q[a]	k_q, 10^7 s^{-1}	N
0.900	0.0180	0.68	32.7
1.25	0.0250	0.65	31.9
1.53	0.0306	0.59	33.4
1.76	0.0352	0.66	31.2
2.15	0.0430	0.61	32.0
	Mean	0.64 ± 0.04	32.2 ± 0.8

[a] Scaled quencher concentration, eq 3.

TABLE 3: Temperature Dependence of the Properties of 50 mM DBNMG Micelles: Aggregation Number, Polarity Index, Microviscosity, and Quencher Rate Constant

T, °C	k_q, 10^7 s^{-1}	N[a]	η, cP	H(25 °C)[b] experimental	H(25 °C)[c] theoretical
21	0.62	33	32 ± 4	0.350 ± 0.005	0.349 ± 0.004
26.5	0.66	42	28 ± 3		0.387 ± 0.003
35	0.89	48	20 ± 2	0.396 ± 0.012	0.411 ± 0.003
45	1.42	49	13.1 ± 0.2	0.410 ± 0.003	0.415 ± 0.003

[a] Relative precision ± 1 molecule. Measured at the scaled quencher concentration of $\eta_Q = 0.025$. Estimated accuracy ± 5%. [b]Equation 19, uncertainty is the standard deviation in 5 measurements. [c]Equation 24, uncertainty due to ±1 molecule relative precision in N.

Table 3 gives the variation of the aggregation number and quencher rate constant as a function of temperature for DBNMG micelles, $X = 1$; Table 4 gives data versus surfactant concentration in DBNMG micelles, $X = 1$; and Table 5 details the results versus micelle composition, X.

TABLE 4: Concentration Dependence of the Aggregation Number and Quencher Rate Constant of DBNMG Micelles. $T = 45$ °C

[DBNMG], mM	k_q, 10^7 s^{-1}	N[a]
50.0	1.42	49
40.0	1.34	48
30.0	1.30	48
20.0	1.29	47

[a] Relative precision ± 1 molecule. Measured at the scaled quencher concentration of $\eta_Q = 0.025$. Estimated accuracy ± 5%.

TABLE 5: Composition Dependence of the Properties of 50 mM DBNMG/SDS Mixed Micelles: Aggregation Number, Polarity Index, Microviscosity, Quencher Rate Constant, Monomer Concentration, Volume in the Polar Shell. $T = 45$ °C

X	k_q, 10^7 s^{-1}	N[a]	[surfactant]$_{free}$, mM	η, cP	V_{shell}, Å^3
1.00	1.43	49.2	0.4	13.1 ± 0.2	2.63×10^3
0.753	1.75	59.5	0.4	11.0 ± 0.1	2.80
0.603	2.25	61.9	0.4	9.6 ± 0.1	2.78
0.356	3.50	63.3	0.6	6.72 ± 0.07	2.69
0.179	5.03	60.8	0.8	4.49 ± 0.06	2.54
0.0000	9.20	48.3	4.9	2.79 ± 0.05	2.14

[a] Relative precision ± 1 molecule. Measure at the scaled quencher concentration of $\eta_Q = 0.025$. Estimated accuracy ± 5%.

The aggregation numbers of DBNMG micelles, $X = 1$, are seen to grow as a function of temperature, remain constant versus surfactant concentration, and vary modestly as a function of mixed micelle composition.

SANS. The scattering data were fit to the same model utilized previously;[8] a charged micelle with a "core−shell" morphology. No ellipticity could be detected,[8] in agreement with the model of eqs 8−10, thus the model was constrained to be a sphere. We had previously followed the common practice of constraining the core radius to be $R_c = 16.7$ Å, the all-trans length of a dodecyl chain.[8] Here we constrain the core radius by adopting the aggregation number derived from the TRFQ results, $N = 49$. Equation 8 gives $R_c = 16.0$ Å.

Figure 3 shows the scattering data together with two fits. The solid line results from fixing the core radius to 16.0 Å in the SANS fitting, yielding a best-fit value for the shell thickness to be $R_m - R_c = 5.8 \pm 0.07$ Å. The dashed line employs $R_c = 16.7$ Å and a best-fit thickness 5.6 ± 0.07 Å. Either of these two fits yields a satisfactory fit to the data.

Theoretical Prediction of the Polarity Index. In this work, we assume therefore a shell thickness of $R_m - R_c = 5.0$ Å for pure SDS micelles[10,25,26] and of $R_m - R_c = 5.8$ Å for pure DBNMG micelles. We further assume that the shell thickness varies linearly as function of micelle composition, i.e.:

$$R_m - R_c = 5.0 + 0.8X \tag{20}$$

This assumption plays no essential role in the conclusions of this paper. The numerical value of the number of water molecules residing in the polar shell and the number of OH bonds interacting with the spin probe depend on eq 20; however, both of these quantities depend more on the absolute value of the polar shell thickness[10] than they do on the dependence depicted by eq 20. Equation 20 is convenient and is within experimental error of the thickness estimated from SANS for all values of X.

The value of the polarity index H(25 °C) in mixed micelles of SDS and DBNMG was previously derived.[10] Equation 16 of ref 10 written in the present notation [$V_{shell} = NV_p$, where V_p was the volume in the polar shell *per surfactant molecule*] is as follows:

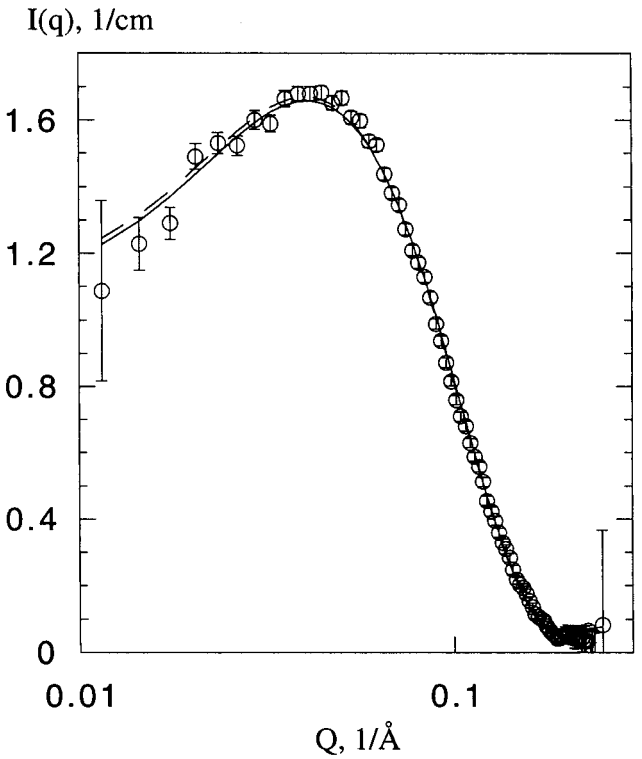

Figure 3. SANS scattering from DBNMG micelles ($X = 1$) at 45 °C. The solid line is the fit to the core-micelle model constraining the radius of the core to $R_c = 16.0$ Å yielding a best-fit shell thickness 5.80 ± 0.07 Å and the dashed line is a fit without this constraint resulting in $R_c = 16.7$ Å and shell thickness 5.60 ± 0.07 Å.

$$H(25\ °C) = 1 - \{nV_{DBNMG} - 30nN_{OH} + (N - n)V_{dry}\}/V_{shell}, \tag{21}$$

where there are n molecules of DBNMG in a mixed micelle of N total surfactant molecules. The volume in the polar shell rendered inaccessible to water by the presence of an SDS molecule is V_{dry} and by a DBNMG molecule is V_{DBNMG}. N_{OH} is the number of OH bonds in the sugar headgroup of DBNMG that contributes to H(25 °C). For a given value of X, there is a distribution of micelles containing 0 to N DBNMG molecules which produces a superposition of EPR spectra. We showed previously[10] that the observed value of A_+, and thus the experimental value of H(25 °C), from this superposition is the same as the average of eq 21. Therefore, since the average value of n is $\langle n \rangle = XN$, the theoretical estimate of the polarity index is as follows:

$$H(25\ °C) = 1 - \{XV_{DBNMG} - 30XN_{OH} + (1 - X)V_{dry}\}N/V_{shell} \tag{22}$$

The number of water molecules per surfactant molecule is then given by

$$N(H_2O) = [V_{shell} - XNV_{DBNMG} - (1 - X)NV_{dry}]/(30N) \tag{23}$$

Equation 23 expresses the fact that volume in the polar shell unoccupied by SDS or DBNMG headgroups is filled with water which has a volume of 30 Å^3.

To compute theoretical values of the polarity index from eq 22, the values of N are taken to be those derived from TRFQ,

Table 5. Values of V_{shell} are calculated from eqs 8 and 9 employing eq 20. The parameter $V_{dry} = 127$ Å^3 is fixed from previous work on SDS and lithium dodecyl sulfate micelles.[25,26] The predicted values of H(25 °C) are sensitive functions of the remaining two parameters, the volume of the sugar headgroup, V_{DBNMG} and the number of OH bonds that are available to interact with the spin probe, N_{OH}. In previous work limited to the region $X < 0.3$, H(25 °C) varied linearly with X; thus we were unable to independently determine V_{DBNMG} and N_{OH}: one more piece of information was needed to separate the two. In the present work, we have three further data points in the region $X > 0.3$, thus this separation may be overdetermined. Due to the profoundly nonlinear behavior of H(25 °C) versus X, this separation may be effected with any one of the three data points, the other two serving as a rather severe test of the hydration model. The best values of $V_{DBNMG} = 580 \pm 10$ Å^3 and $N_{OH} = 7.4 \pm 0.2$ were found by minimizing the least-squares difference between the experimental values and those of eq 22. The value of $N(H_2O)$ in eq 23 becomes negative for $X = 1$. In this case, the volume of the headgroups exceeds the shell volume, so $N(H_2O)$ is set equal to zero, and

$$H(25\ °C) = 30N_{OH}\,N/V_{shell} \qquad (24)$$

The predictions of eq 22 are plotted as circles in Figure 1. The uncertainties indicated by the error bars on the theoretical values of H(25 °C) are the uncertainties due to V_{DBNMG} and N_{OH} added in quadrature. We emphasize that the absolute values of V_{dry}, V_{DBNMG}, and N_{OH} all depend on the chosen value of the shell thickness.

Figure 4 shows the number of water molecules per surfactant molecule (left-hand ordinate) versus micelle composition, eq 23. The error bars reflect the uncertainty in the value of V_{DBNMG}. Again, uncertainty in the shell thickness dominates the uncertainty in $N(H_2O)$. For example, an uncertainty of ±0.8 Å in the thickness, leads to an uncertainty in $N(H_2O)$ of ±3 molecules at $X = 0$ and ±2 molecules at $X = 1$. Note the uncertainty in the use of eq 20 falls within the overall uncertainty in the shell thickness. In the same figure, Figure 4, the shell volume is plotted (right-hand ordinate) versus micelle composition showing that this volume varies only modestly (standard deviation about the mean 9.3%) over the full concentration range. The lines are to guide the eye.

Values of A_+ were measured at 45 °C in pure DBNMG at concentrations of [DBNMG] = 20, 30, 40, and 50 mM. From these, experimental values of the polarity index were derived from eq 19 and found to be constant at H(25 °C) = 0.411 ± 0.003, where the uncertainty is the standard deviation in 20 measurements, 5 at each concentration. A constant theoretical value of H(25 °C) = 0.407 ± 0.004 is computed from eq 24 keeping the same parameters $V_{DBNMG} = 580$ Å^3 and $N_{OH} = 7.4$ employed in Figure 1. The uncertainty is the standard deviation due to the variation in N in column 3 of Table 4. Similarly, values of H(25 °C) were found as a function of the temperature. These, together with the theoretical values are reported in Table 3, again keeping $V_{DBNMG} = 580$ Å^3 and $N_{OH} = 7.4$. The experimental and theoretical values are in excellent agreement. Notably, the polarity index increases in pure DBNMG micelles as a function of the aggregation number; opposite the result in SDS[25] and LiDS[26] micelles. The reason for this difference is due to the source of the OH bonds. In SDS and LiDS micelles, as the micelles increase in size, the available volume for water per surfactant molecule is decreased, leading to a decrease in polarity. In pure DBNMG micelles, there is no water. A decrease in available volume per surfactant molecule increases the volume density of OH bonds from the sugar groups leading to the increase in polarity.

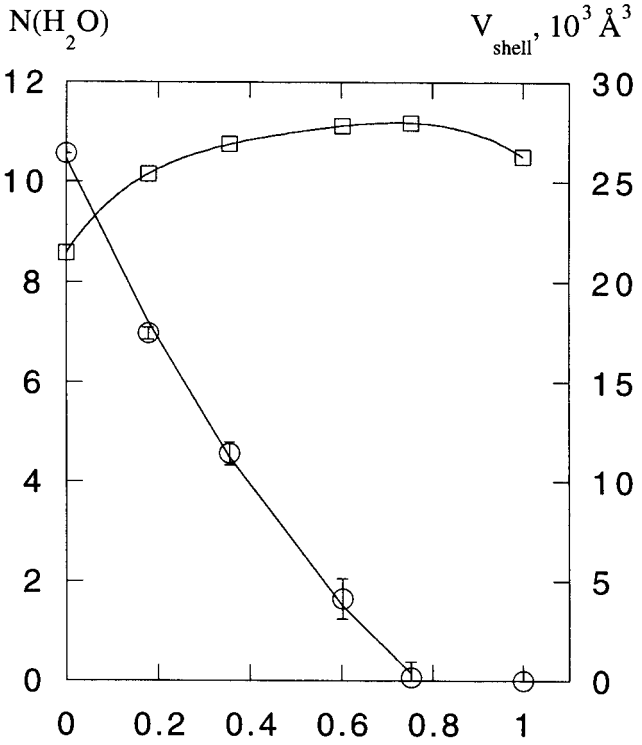

Figure 4. Number of water molecules per surfactant molecule, circles (left-hand ordinate) and the volume in the polar shell, squares (right-hand ordinate) in mixed micelles versus micelle composition. The lines are to guide the eye. The error bars are due to the uncertainties in V_{DBNMG} and N_{OH} added in quadrature reflecting the relative uncertainty in values of $N(H_2O)$. $N(H_2O)$ becomes formally zero at $X = 0.75$ where the volume of the sugar headgroups exceeds the available volume in the polar shell.

Discussion

Figures 1 and 2 show that the polar shell of mixed micelle SDS/DBNMG presents a polarity and microviscosity that are tunable over a considerable range by adjusting the composition, X. The hydration is given by Figure 4 which shows that the number of water molecules per surfactant varies from about 10 at $X = 0$ to near zero above $X = 0.75$. From the data in Figure 1 alone, uncertainties in the polar shell thickness could admit up to approximately 2 molecules of water per surfactant up to $X = 1$; however, the temperature dependence of H(25 °C), Table 3, supports a model of very little water in the polar shell above $X = 0.75$. The value of H(25 °C) increases with aggregation number as the temperature is raised, Table 3. Even very small amounts of water in the polar shell would lead to the opposite trend because if water contributes significantly to H(25 °C), then, as the micelle grows, the expulsion of this water would decrease the value of H(25 °C). We find that even an average of 0.25 molecules of water per surfactant molecule residing in the polar shell at 45 °C would reverse the trend shown in Table 3. It is important to understand that a dry micelle does not imply that an additive molecule residing in the polar shell of a DBNMG micelle would not come into contact with water. The probe probably exercises excursions into the core and into the water phase. For example, if the probe briefly diffuses into the core with a probability of 0.63 and into the aqueous phase with a probability of 0.37, this would leave the value of H(25 °C) unchanged at 0.37. Obviously, such excursions would change

the average polarity sensed by the probe; however, the excellent overall agreement between theory and experiment here and in previous work[25,26] supports the model in which the preponderance of the contribution to the value of H(25 °C) is due to the polar shell.

The error bars in Figure 4 are indicative of the uncertainty in the relative values of water content; thus, the relative water content can be adjusted with considerable precision. Near $X = 0$, the aggregation numbers and therefore the number of water molecules per surfactant may be varied considerably by adding salt or by varying the surfactant concentration.[25] Thus different ranges of water content may be achieved.

The simple hydration model of eq 22 and, in the absence of water in the polar shell, eq 24, correctly predicts a decrease in the polarity index from $X = 0$ to about $X = 0.75$ where it goes through a minimum and then increases. The essentially perfect agreement in Figure 1 is achieved without adding any more parameters to those introduced in earlier work.[25,26] The parameter V_{dry} was held fixed in SDS[25] and LiDS[26] micelles as the aggregation numbers in these surfactants were increased by adding either salt or surfactant. The parameters V_{DBNMG} and N_{OH} were found to depend linearly on one another in earlier work[10] on DBNMG/SDS micelles at $X < 0.3$. To reproduce the experimental data in Figure 1, both of these parameters are held fixed to within rather stringent limits. We emphasize that the absolute values of these parameters depend on the volume of the polar shell, V_{shell}, eq 9, where the shell thickness is presently taken to be given by eq 20. The fact that the model yields excellent agreement with experiment is not affected by this choice. For example, equally good agreement is achieved in Figure 1 by assuming a shell thickness that varies from 4.4 to 5.2 Å^3 from $X = 0$ to 1; however, in this case, $V_{dry} = 99$ Å^3, $V_{DBNMG} = 560$ Å^3, and $N_{OH} = 7.4$. Thus, the numerical values of these parameters depend somewhat on the shell thickness. For any reasonable choice of shell thickness, V_{DBNMG} is of the same order of magnitude as the volume computed from molecular models,[10] 524 Å^3.

If it is indeed true that the polar shell of DBNMG micelles are dry, then this polar shell presents an interesting liquid indeed; it is a liquid of sugar molecules with no lubricating water. It is a viscous liquid; $\eta = 13.1$ cP at 45 °C increasing to about 30 cP at 21 °C.

The decrease in H(25 °C) from $X = 0$ to near $X = 0.75$ is due to the more rapid decrease in OH bonds from expelled water than the increase in OH bonds brought in by added sugar headgroups. In this composition region, the sugar headgroups physically expel water molecules amounting to 580 Å^3/30 Å^3 = 19 molecules of water for each molecule of DBNMG. Near $M = 0.75$, the micelle becomes rather dry. Then, the increase in H(25 °C) is due to the increase in sugar groups bringing in more OH bonds. The number of OH bonds per DBNMG interacting with the spin probe is held constant at 7.4 compared with the maximum number possible, 10.

Figure 5 shows a plot of the quenching rates of pyrene by DMBP taken from Tables 3 and 5 versus the values of C_QT/η, where the viscosity is taken from EPR rotational correlation times corrected for micelle rotation as tabulated in Tables 3 and 5. The straight line is a least-squares fit to eq 18 yielding a quenching probability of $P = 0.5$ with a coefficient of correlation $r = 0.997$. The error bars reflect the uncertainties in the viscosity determined by EPR. In this case, the Stokes−Einstein equation provides an excellent hydrodynamic description of fluorescence quenching in mixed micelles whether the viscosity is varied (by varying the composition) or if the temperature (and therefore the viscosity) is varied. There is a modest variation in the molar concentration of quencher, C_Q, due to the ±9.3% standard deviation in the polar shell volume about its mean value (Figure 4, right-hand ordinate). Failure to include this variation in the computation of quenching rate, eq 18, results in a poorer fit than that shown in Figure 5, especially for the data derived from temperature variation. A far better test of the dependence of k_q on the volume of the polar shell will come from micelles in which the aggregation number can be varied over a wider range.

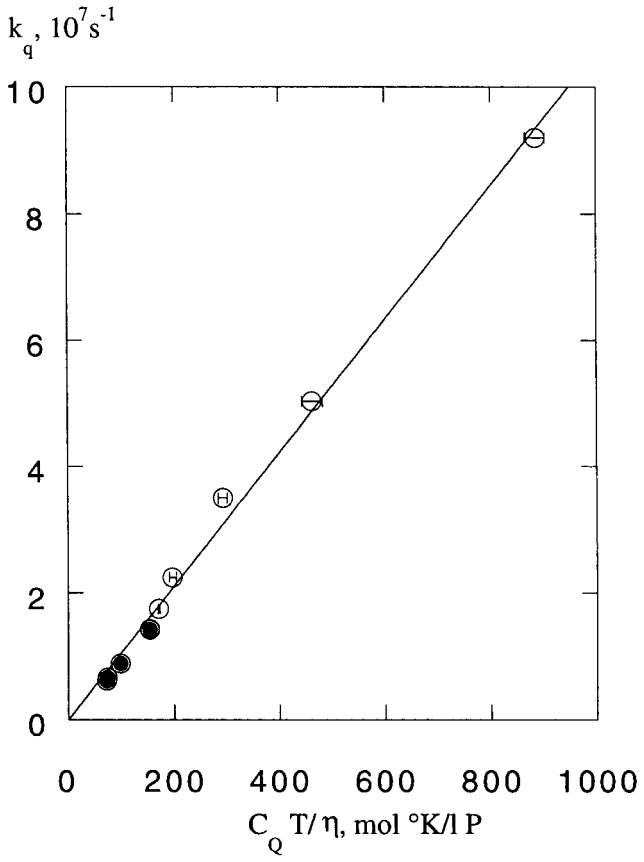

Figure 5. The fluorescence quenching rate of pyrene by dimethyl benzophenone versus C_QT/η for micelles of varying composition at 45 °C, ○, and for DBNMG micelles at varying temperatures (21.5 to 45 °C), ●. The straight line is a linear least-squares fit of all of the data to the Stokes−Einstein equation, eq 18, yielding a probability of quenching per collision $P = 0.5$. The molar concentration C_Q is due to one quencher in the volume defined by the polar shell and the viscosity is determined by the rotational motion of a nitroxide spin probe.

Note that the value of $P = 0.5$ results from the fact that we have assumed that the polar shell thickness taken from SANS measurements, eq 20, is the same as that bounding the diffusional motion of pyrene and DMBP. We further assume that the microviscosity estimated from the rotation of the spin probe is the appropriate viscosity to use in eq 18. This, in turn, assumes that the spin probe reports an average viscosity over the same volume occupied by pyrene and DMBP. If, in fact, the effective volumes from the SANS measurements and for the motion of the various probes are somewhat different, the numerical value of P would be altered. For example, introducing an uncertainty in the shell thickness of ± 0.8 Å results in uncertainty in P of ± 0.1; i.e., about 20%. It is important to note that altering the shell thickness does not affect the linearity of the curve in Figure 5, only the slope is changed. In other the words, the Stokes−Einstein equation is valid in any case.

Conclusions

By combining three techniques it is possible to construct a rather complete picture of the mixed micelles of SDS and DBNMG viewed as a variable reaction medium. The water content may be varied from about 10 molecules per surfactant to near zero while the viscosity can be controlled over about a factor of 5 at a constant temperature of 45 °C. The Stokes−Einstein law provides an excellent hydrodynamic description of the bimolecular collision rates of pyrene and dimethyl benzophenone as these molecules execute diffusional motion throughout the polar shell.

Acknowledgment. We gratefully acknowledge support from NIH/MBRS S06 GM48680-03, EPSRC, the ISIS facility, Kodak Research and Development, the CSUN Research and Grants Committee, and the CSUN College of Science and Mathematics. We thank A. M. Howe and A. R. Pitt of Kodak European R&D for a generous gift of DBNMG. One of the authors (R.R.) thanks Mats Almgren for hosting a visit to Uppsala University where the TRFQ measurements were conducted. This visit was supported by NIH GM00667-0.

References and Notes

(1) Soten, I.; Ozin, G. A. *Curr. Opin. Colloid Interface Sci.* **1999**, *4*, 325.
(2) Grieser, F.; Drummond, C. J. *J. Phys. Chem.* **1988**, *92*, 5580.
(3) Shiloach, A.; Blankschtein, D. *Langmuir* **1998**, *14*, 1618.
(4) Desai, T. R.; Dixit, S. G. *J. Colloid Interface Sci.* **1996**, *177*, 471.
(5) Kronberg, B. *Curr. Opin. Colloid Interface Sci.* **1997**, *2*, 456.
(6) Hill, R. M. In *Mixed Surfactant Systems*; Ogina, K., Abe, M., Eds.; Marcel Dekker: New York, 1993; p 317.
(7) Abe, M.; Ogino, K. In *Mixed Surfactant Systems*; Ogina, K., Abe, M., Eds.; Marcel Dekker: New York, 1993; p 1.
(8) Griffiths, P. C.; Whatton, M. L.; Abbott, R. J.; Kwan, W.; Pitt, A. R.; Howe, A. M.; King, S. M.; Heenan, R. K. *J. Colloid Inter. Sci.* **1999**, *215*, 114.
(9) Griffiths, P. C.; Stilbs, P.; Paulson, K.; Howe, A. M.; Pitt, A. R. *J. Phys. Chem.* **1997**, *101*, 915.
(10) Bales, B. L.; Howe, A. M.; Pitt, A. R.; Roe, J. A.; Griffiths, P. C. *J. Phys. Chem.* **2000**, *104*, 264.
(11) Holland, P. M.; Rubini, P. In *Mixed Surfactant Systems: An Overview*; M., H. P., Rubingh, D. N., Eds.; American Chemical Society: Washington, DC, 1996.
(12) Scamehorn, J. F. In *Phenomena in Mixed Surfactant Systems*; Scamehorn, J. F., Ed.; American Chemical Society: Washington, DC, 1996.
(13) Bales, B. L.; Almgren, M. *J. Phys. Chem.* **1995**, *99*, 15153.
(14) Infelta, P. P.; Grätzel, M.; Thomas, J. K. *J. Phys. Chem.* **1974**, *78*, 190.
(15) Tachiya, M. *Chem. Phys. Lett.* **1975**, *33*, 289.
(16) Gehlen, M. H. *Chem. Phys. Lett.* **1993**, *212*, 362.
(17) Quina, F. H.; Nassar, P. M.; Bonilha, J. B. S.; Bales, B. L. *J. Phys. Chem.* **1995**, *99*, 17028.
(18) Rubingh, D. N. In *Solution Chemistry of Surfactants*; Mittal, K., Ed.; Plenum: New York, 1979; Vol. 1.
(19) Halpern, H. J.; Peric, M.; Yu, C.; Bales, B. L. *J. Magn. Reson.* **1993**, *103*, 13.
(20) Bales, B. L. Inhomogeneously Broadened Spin-Label Spectra. In *Biological Magnetic Resonance*; Berliner, L. J., Reuben, J., Eds.; Plenum Publishing Corporation: New York, 1989; Vol. 8, p 77.
(21) Schreier, S.; Polnaszek, C. F.; Smith, I. C. P. *Biochim. Biophys. Acta* **1978**, *515*, 375.
(22) Bales, B. L.; Stenland, C. *J. Phys. Chem.* **1993**, *97*, 3418.
(23) Gaffney, B. J.; McConnell, H. M. *J. Magn. Res.* **1974**, *16*, 1.
(24) Jost, P.; Libertini, L. J.; Hebert, V. C.; Griffith, O. H. *J. Mol. Biol.* **1971**, *59*, 77.
(25) Bales, B. L.; Messina, L.; Vidal, A.; Peric, M.; Nascimento, O. R. *J. Phys. Chem.* **1998**, *102*, 10347.
(26) Bales, B. L.; Shahin, A.; Lindblad, C.; Almgren, M. *J. Phys. Chem.* **2000**, *104*, 256.
(27) Lindman, B.; Wennerström, H.; Gustavsson, H.; Kamenka, N.; Brun, B. *Pure Appl. Chem.* **1980**, *52*, 1307.
(28) Tanford, C. *The Hydrophobic Effect: Formation of Micelles and Biological Membrane*, 2nd ed.; Wiley-Interscience: New York, 1980.
(29) Jones, L. L.; Schwartz, R. N. *Mol. Phys.* **1981**, *43*, 527.
(30) Bondi, A. *J. Phys. Chem.* **1964**, *68*, 441.
(31) Wikander, G.; Johansson, L. B.-Å. *Langmuir* **1989**, *5*, 728.
(32) Debye, P. *Trans. Electrochem. Soc.* **1942**, *82*, 265.
(33) North, A. M. *The Collisional Theory of Chemical Reactions in Liquids*; John Wiley: New York, 1964.
(34) Molin, Y. N.; Salikhov, K. M.; Zamaraev, K. I. *Spin Exchange. Principles and Applications in Chemistry and Biology*; Springer-Verlag: New York, 1980; Vol. 8.
(35) Almgren, M. Kinetics of Excited-State Processes in Micellar Media. In *Kinetics and Catalysis in Microheterogeneous Systems*; Grätzel, M., Kalyanasundaram, K., Eds.; Marcel Dekker: New York, 1991; p 63.
(36) Mukerjee, P.; Ramachandran, C.; Pyter, R. A. *J. Phys. Chem.* **1982**, *86*, 3189.
(37) León, V.; Bales, B. L.; Viloria, F. *Mol. Cryst. Liq. Cryst. Lett.* **1980**, *56*, 229.
(38) Yoshioka, H. *J. Am. Chem. Soc.* **1979**, *101*, 28.
(39) Vargaftik, N. B. *Tables on the Thermophysical Properties of Liquids and Gases*, 2nd ed.; Hemisphere Publishing: Washington, 1975; Vol. 4. (English Translation)
(40) Yoshioka, H. *J. Colloid Interface Sci.* **1978**, *66*, 352.
(41) Ranganathan, R.; Peric, M.; Bales, B. L. *J. Phys. Chem.* **1998**, *102*, 8436.